

Supplementary Information

Cooling Growth of Millimeter-Size Single-Crystal Bilayer Graphene at Atmospheric Pressure

Haibin Sun^{†,‡}, Yan Han[†], Jun Wu[†], Yang Lu[‡], Junqi Xu[‡], Yongsong Luo[‡], Fengqi Song^{†,§},

Guanghou Wang^{†,§}, Jianguo Wan^{*,†,§}

[†]National Laboratory of Solid State Microstructures and Department of Physics, Nanjing University, Nanjing 210093, China

[‡]Key Laboratory of Advanced Micro/Nano Functional Materials, Department of Physics and Electronic Engineering, Xinyang Normal University, Xinyang 464000, China

[§]Collaborative Innovation Center of Advanced Microstructures, Nanjing University, Nanjing 210093, China

*Corresponding author (wanjg@nju.edu.cn)

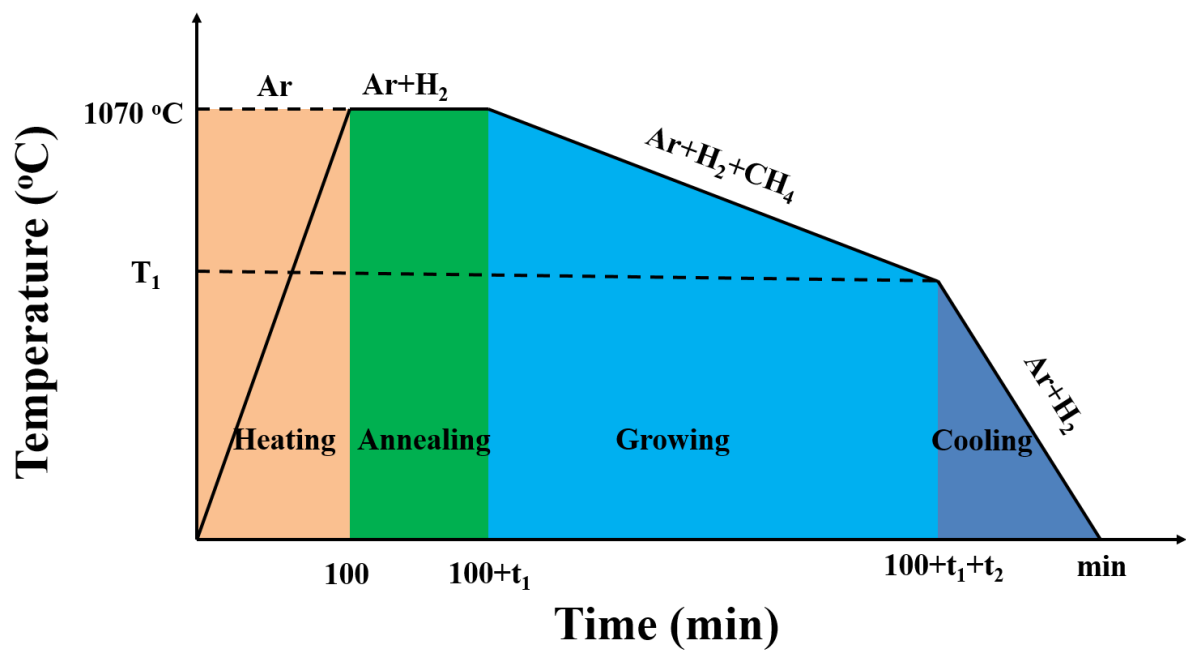


Figure S1. NI-APCVD growth process and experimental parameters for bilayer graphene production. A systematic study on nucleation density and synchronization growth property dependence on the different annealing duration (t_1), cooling growth duration (t_2) and cooling temperature (T_1). The plot profile shows growth stage for the growth processes with variable annealing duration (t_1) (see Fig. 2), for variable cooling temperature (T_1) with variable cooling growth duration (t_2) (see Fig. 3) in Ar/H₂ before ramping up to 1070 °C in Ar only for growth.

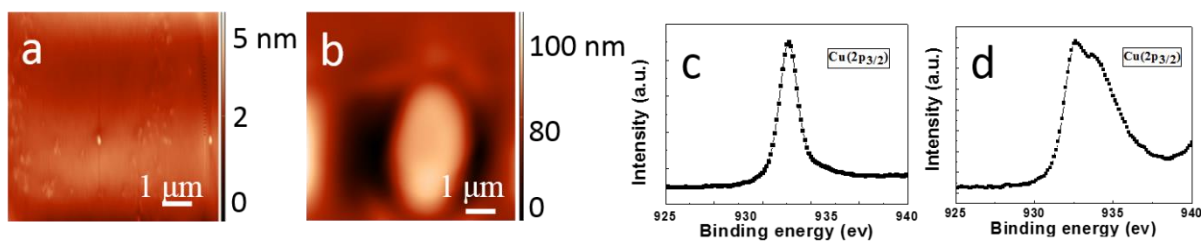


Figure S2. Morphology characterization of preheating Cu foils with Ar/H₂ and Ar-only.

AFM images of Cu foils preheated in Ar/H₂ mixture (a) and in Ar-only (b). Cu 2P_{3/2} XPS spectra for Cu foils preheated in Ar/H₂ mixture (c) and in Ar-only (d). Preheated Cu foils showed a rather high roughness surface with a surface decorated nanoparticles, which proved that Cu foils have been oxidized after heating in Ar.

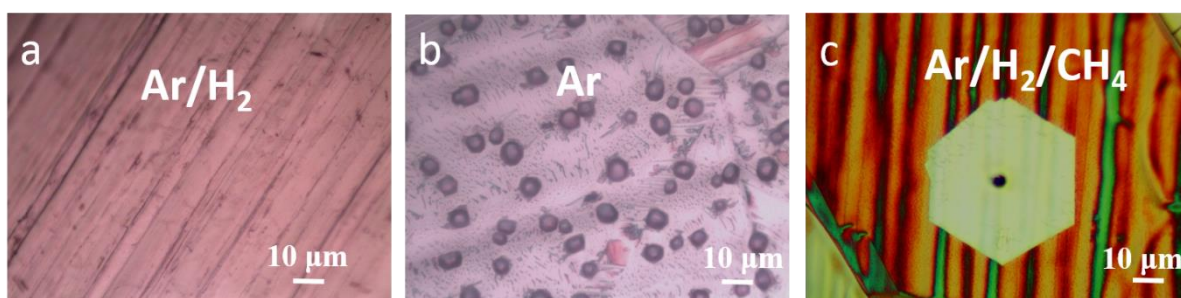


Figure S3. Optical microscope images of preheating Cu foils. (a) Preheated in Ar/H₂ mixture. (b) Preheated in Ar-only. (c) Graphene nucleation with the Cu₂O particle in the center.

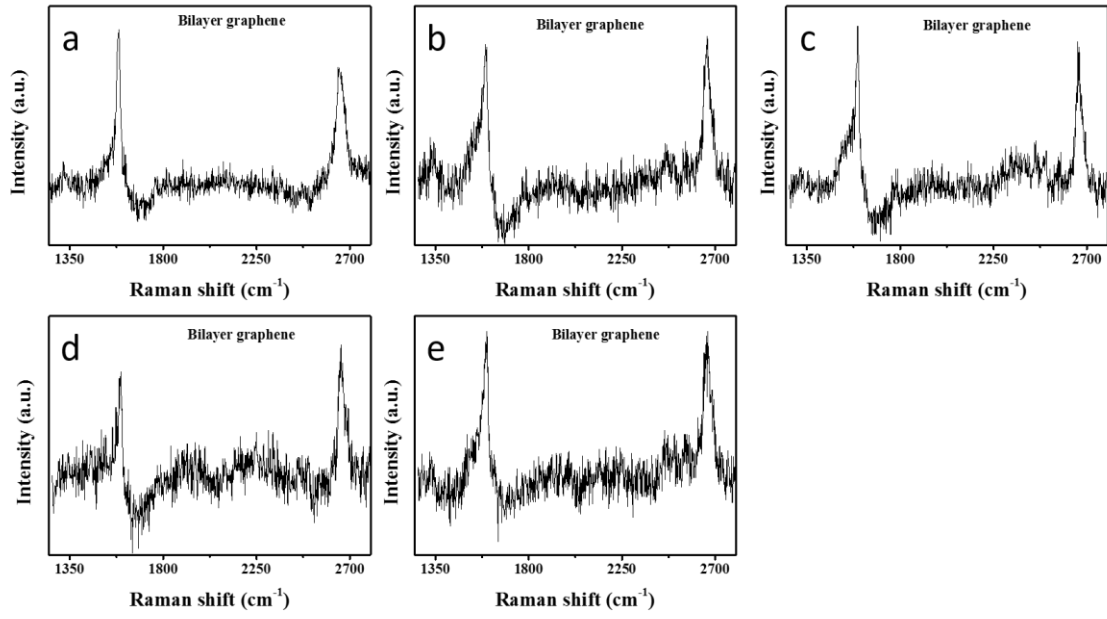


Figure S4. Raman spectroscopy characterization of graphene grains. (a-e) Raman spectra obtained from the SEM images in Fig 2 (c-g), there is a one-to-one correspondence between Raman spectra and SEM images, indicating that all samples are the bilayer graphene.

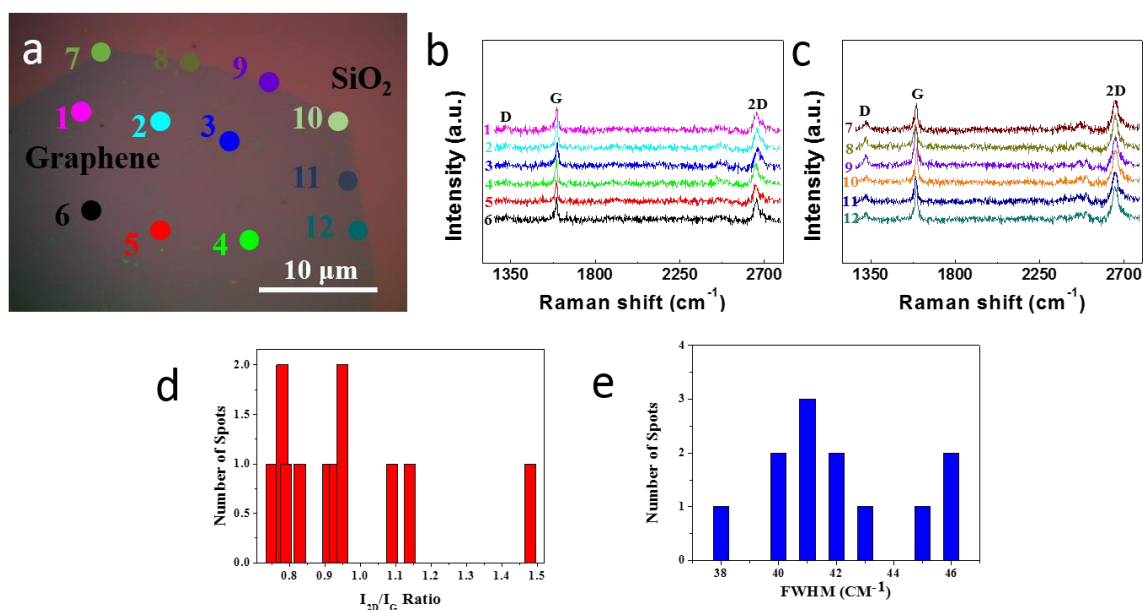


Figure S5. Raman spectroscopy characterization of the large-scale single-crystal graphene grain. (a) Optical microscope image of the graphene crystallite transferred to a SiO_2/Si substrate. (b-c). Color-coded stacked Raman spectra corresponding to the spots identified in a. (d-e) Histograms of the Raman spectrum I_{2D}/I_G ratio and 2D band fwhm values of the bilayer graphene.

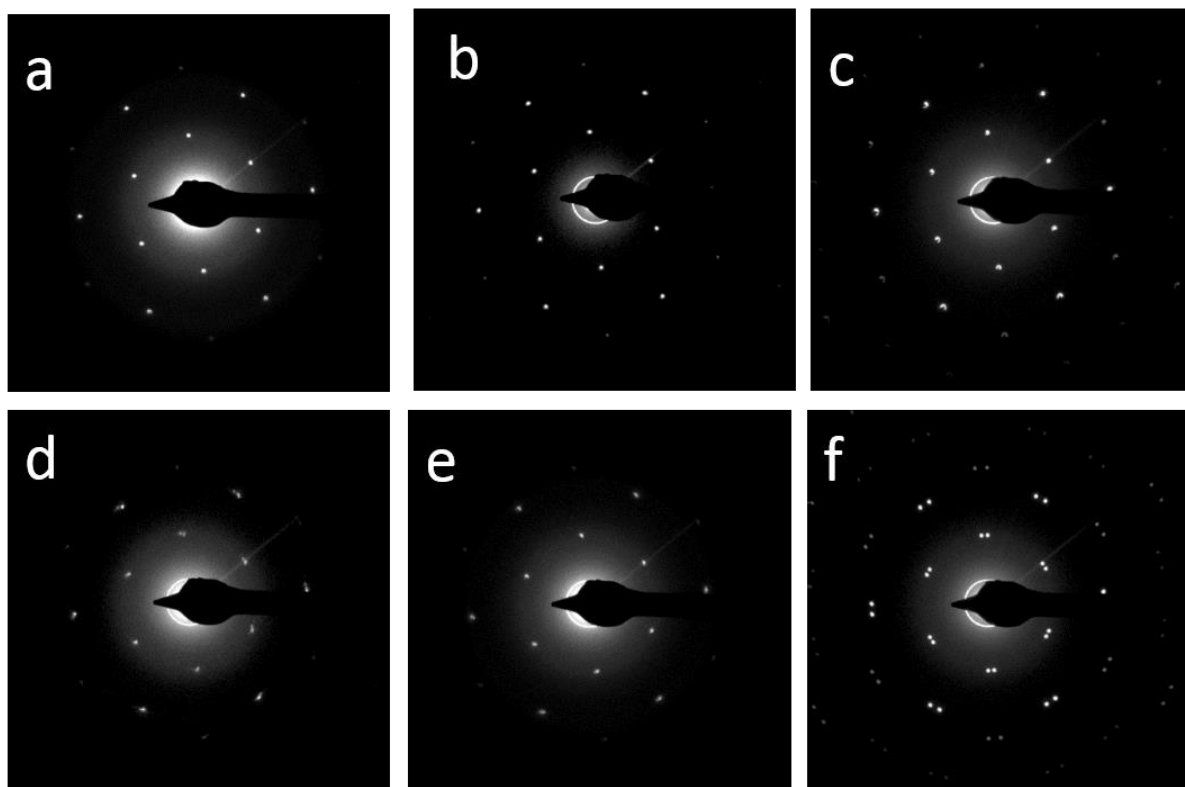


Figure S6. SAED characterization of graphene grains. (a-f) SAED patterns taken in different windows of the TEM grid, as shown in Fig 4e, and demonstrate that these points have the same orientations.

Table S1. Comparison of the synthesis method and structure properties of single-crystal bilayer graphene domains obtained by CVD.

	Substrate	Temperature (°C)	Pressure	Synthesis method	Size (μm)	Shape	Reference
1	Cu	1050	Low	High temperature and low pressure of two-step CVD process	20	Hexagon	Acs Nano, 2012 ⁷
2	Cu	1030	Low	Reduce the flow rate ratio of H ₂ /CH ₄ to keep lower growth rate	410	Flower	Nano Lett, 2013 ¹⁶
3	Cu	1070	Low	Maintain a Cu ₂ O layer and reduce the flow rate ratio of H ₂ /CH ₄	300	Hexagon	Nat. Commun, 2013 ¹⁷
4	Cu	1050	Ambient	Oxidize the Cu surface to form Cu ₂ O nanoparticles as the growth seeds	540	Hexagon	Nanoscale, 2015 ¹⁸
5	O-rich Cu	1035	Low	Oxygen-activated CVD process	500	Hexagon	Nat. Nanotechnol, 2016 ³³
6	Cu	1070	Ambient	Oxidize the Cu surface and the following nonisothermal growth process	1000	Hexagon	This manuscript

Table S2. Summary of Raman spectra of graphene growth from the different synthesis methods.

Number	Substrate	G/2D ratio	D/G ratio	Synthesis method	Layer
1	Graphene/SiO ₂ /Si	1.1	0.02	Fig. 1(c)	Bilayer graphene
2	Graphene/SiO ₂ /Si	1.2	0.10	Fig. 1(e)	Bilayer graphene
3	Graphene/SiO ₂ /Si	1.0	0.04	Fig. 1(f)	Bilayer graphene
4	Graphene/SiO ₂ /Si	0.8	0.08	Fig. 1(g)	Bilayer graphene
5	Graphene/SiO ₂ /Si	1.3	0.07	Fig. 2(c)	Bilayer graphene
6	Graphene/SiO ₂ /Si	0.9	0.08	Fig. 2(d)	Bilayer graphene
7	Graphene/SiO ₂ /Si	1.1	0.08	Fig. 2(e)	Bilayer graphene
8	Graphene/SiO ₂ /Si	0.8	0.05	Fig. 2(f)	Bilayer graphene
9	Graphene/SiO ₂ /Si	1.0	0.06	Fig. 2(g)	Bilayer graphene
10	Graphene/SiO ₂ /Si	0.9	0.08	Fig. 3(a)	Bilayer graphene
11	Graphene/SiO ₂ /Si	1.4	1.0	Fig. 3(b)	Multilayer graphene
12	Graphene/SiO ₂ /Si	1.1	0.06	Fig. 3(c)	Bilayer graphene

13	Graphene/SiO ₂ /Si	1.1	0.05	Fig. 3(d)	Bilayer graphene
14	Graphene/SiO ₂ /Si	1.7	0.08	Fig. 3(e)	Multilayer graphene
15	Graphene/SiO ₂ /Si	1.3	0.08	Fig. 3(f)	Bilayer graphene
16	Graphene/SiO ₂ /Si	1.1	0.04	Fig. 3(g)	Bilayer graphene
17	Graphene/SiO ₂ /Si	1.0	0.08	Fig. 3(h)	Bilayer graphene
18	Graphene/SiO ₂ /Si	1.3	0.02	Fig. S5-1	Bilayer graphene
19	Graphene/SiO ₂ /Si	1.3	0.02	Fig. S5-2	Bilayer graphene
20	Graphene/SiO ₂ /Si	1.3	0.02	Fig. S5-3	Bilayer graphene
21	Graphene/SiO ₂ /Si	1.2	0.02	Fig. S5-4	Bilayer graphene
22	Graphene/SiO ₂ /Si	1.1	0.02	Fig. S5-5	Bilayer graphene
23	Graphene/SiO ₂ /Si	1.1	0.02	Fig. S5-6	Bilayer graphene
24	Graphene/SiO ₂ /Si	1.3	0.08	Fig. S5-7	Bilayer graphene
25	Graphene/SiO ₂ /Si	1.1	0.08	Fig. S5-8	Bilayer graphene
26	Graphene/SiO ₂ /Si	0.9	0.08	Fig. S5-9	Bilayer graphene

27	Graphene/SiO ₂ /Si	0.9	0.08	Fig. S5-10	Bilayer graphene
28	Graphene/SiO ₂ /Si	0.7	1.0	Fig. S5-11	Bilayer graphene
29	Graphene/SiO ₂ /Si	1.1	0.08	Fig. S5-12	Bilayer graphene